

**CY2022 Annual Report N00014-19-1-2254**

Final Report

**Prof. Jorge Rocca**

**Colorado State University**

**Grant or Contract Number:** Office of Naval Research Award N00014-19-1-2254

**Project Title:** “Generation and Atmospheric Propagation of High Energy Ultrashort Pulses at High Repetition Rate”

**Final Report:** CY2022

**Principle Investigator:** Jorge Rocca, 970-491-8371, [jorge.rocca@colostate.edu](mailto:jorge.rocca@colostate.edu)  
Colorado State University

This work was sponsored by the Office of Naval Research (ONR), under grant (or contract) number N00014-19-1-2254. The views and conclusions contained herein are those of the authors only and should not be interpreted as representing those of ONR, the U.S. Navy or the U.S. Government.

1. **DISTRIBUTION STATEMENT:** A. Approved for public release distribution unlimited.

## 2. ACCOMPLISHMENTS

### • 2.1 Major Goals and Objectives of the Project :

Defense applications in directed energy, such as channeling of intense laser and microwave beams and guiding of electrical discharges in the atmosphere, x-ray and gamma ray generation, remote sensing, and others will greatly benefit from the availability of efficient high energy ultrashort pulse lasers capable of delivering Joule and multi-Joule-level pulses at kHz repetition rates (kW average powers). Presently, Joule-level picosecond and femtosecond lasers are mostly limited to repetition rates of 10 Hz. Moreover, since these lasers are typically pumped by flashlamps, these lasers are large in size, inefficient, and non-portable. Consequently, studies of Joule-level energy laser pulse propagation in the atmosphere have been mostly limited to low repetition rates. A new high average power, high energy, picosecond diode-pumped Yb:YAG laser technology was demonstrated at Colorado State University achieving for example 1.1 J of a few picosecond duration train of pulses at 1000 Hz or 1,100 W average power (Optics Letters 2020), that is scalable to multi-kW average power.

A goal of this project was to gain understanding of the propagation of high energy (Joule-level) picosecond laser pulses generated at repetition rates up to 1 kHz in air and kW-level average powers. This includes the study of laser filamentation in this new regime, in which the short time separation between contiguous laser pulses causes the filamentation of a pulse to be affected by the atmospheric density depression caused by the preceding pulses. These studies include experiments that use these laser filaments to guide electrical discharge channels in the atmosphere at repetition rates up to 1 kHz. Another goal of the project is to extend high energy kHz repetition rate laser capability to the femtosecond range by using our diode-pumped cryogenic Yb:YAG laser technology to pump a high average power Ti:Sapphire laser. This laser would allow for similar atmospheric beam propagation studies to be conducted with high energy femtosecond pulses.

### 2.2 What was accomplished towards these goals :

One of the major tasks conducted during the last year of the project related to the laser filament guiding of electrical discharges in the atmosphere at 1 kHz repetition rate using high energy picosecond laser pulses. Laser induced filaments have been shown to significantly reduce the voltage necessary to initiate electric discharges in atmospheric air and can guide their propagation over long distances. The majority of the laser-guided discharge studies have been conducted at repetition rates of 10 Hz, where the medium completely recovers before the next laser pulse arrives, and with low energy laser pulses. We demonstrate the stable generation of laser filament-guided electric discharge columns in air at up to 1 kHz repetition rate, and report on the physics of discharges initiated by high energy (up to 250 mJ) 1030 nm wavelength laser pulses of 7 ps duration at repetition rates up to 1 kHz. A current proportional to the laser pulse energy is observed as soon as the laser pulse arrives, initiating a high impedance phase of the discharge. Full breakdown, characterized by impedance collapse and the onset of high current conduction, occurs 100s of ns to a few  $\mu$ s later. A record  $\sim 4.2 \times$  reduction in breakdown voltage for dc-biased discharges is

observed to result dominantly from the perturbation caused by a single laser pulse, with cumulative effects playing only a secondary role. The gaps between the filamentary plasma channel and the electrodes are shown to play a role in the breakdown delay. The increased understanding of kHz repetition rate filament-guided discharges can aid the use in applications.

Another goal of this project was to extend high energy kHz repetition rate laser capability to the femtosecond range by using our diode-pumped cryogenic Yb:YAG laser technology to pump a high average power Ti:Sapphire laser. In major milestone achieved we generated J green pulses ( $\lambda=515$  nm) at a record repetition rate of 1 kHz . A fraction of the power from this new 1 KHz repetition rate green was used to pump the first stage of amplification of the proposed Ti:Sapphire laser system. We demonstrated a side-pumped cross-seeded thin-slab pre-amplifier for high-power Ti:Sa laser systems. This room temperature Ti:Sa amplifier uses a cross pump-seed geometry to generate 30mJ output pulses at 0.5 kHz repetition rate, and 25mJ at 1 kHz when pumped by 100 mJ  $\lambda=515$ nm pump from the diode pumped Yb:YAG laser. The crystal geometry allows to maintain the crystal at  $\sim 30$  C with a water-cooling temperature of 10 C. The amplifier is an attractive solution for use in the first stages of amplification in high peak and high average power chirped pulse amplification laser systems.

The accomplishments reached during the last year of the project are summarized below.

### **2.2.1 Atmospheric filamentation of high energy picosecond laser pulses at 1000 Hz repetition rates.**

Earlier in the project, laser-driven plasma filaments, using repetition rates up to 1000 Hz and individual laser pulse energies up to 200 mJ. This is a new regime, in which the short time separation between contiguous laser pulses causes the filamentation of a pulse to be affected by the atmospheric density depression caused by the preceding pulses. We completed the analysis of the data obtained and published the results in Optics Letters in December 2021: A. Higginson, Y. Wang, H. Chi, A. Goffin, I. Larkin, H.M. Milchberg, and J.J. Rocca, “Wake dynamics of air filaments generated by high-energy picosecond laser pulses at 1 kHz repetition rate”, Optics Letters, 46, 5449, (2021)

### **2.2.2 .Laser filament guiding of electrical discharges in air at 1 kHz repetition rate**

During the last year of the of the project we conducted experiments that used these laser filaments to guide electrical discharge channels in the atmosphere at repetition rates up to 1 kHz. Laser induced filaments can significantly reduce the voltage necessary to initiate electric discharges in air and guide their propagation, opening paths to applications. The majority of the previous laser-guided discharge studies have been limited to repetition rates of 10 Hz, where the medium completely recovers before the next laser pulse arrives. During the current reporting period we have studied of the physics of laser filament-guided electric discharges in atmospheric air at repetition rates up to 1 kHz initiated by high energy (up to 250 mJ) 1030 nm wavelength laser pulses of 7 ps duration, using optical diagnostics, electrical measurements, and modeling. A breakdown voltage reduction of up to 4.5 X is achieved between parallel electrodes with axial holes sustaining a nearly uniform field. The breakdown voltage reduction results dominantly from the perturbation caused by a single laser pulse, with cumulative effects playing only a secondary role. As soon as the laser pulse arrives a flow of current proportional to the laser pulse energy is initiated through a high impedance plasma. Full breakdown, characterized by impedance collapse and the onset of high current conduction, occurs 100s of ns to a few  $\mu$ s later in the absent of streamers propagating along

the filament channel. The gaps between the filament channel and the electrodes play a role in the breakdown delay. The major conclusions are summarized below, and the results are described in more detail in Appendix A.

1. Laser filaments generated by high energy picosecond pulses are observed to reduce breakdown voltage by 4.2 X.
2. Discharge channels are observed to be free of streamers.
3. Large pre-current (greater,  $> 10$ 's mA) is observed to precede discharge breakdown.
4. Discharge breakdown was observed to be independent of repetition rate. This suggests that the effect of single laser pulse dominates over cumulative density depression created by preceding laser pulses.

### **2.2.3 Demonstration of a side-pumped cross-seeded thin-slab pre-amplifier for high power Ti:Sapphire laser system**

Another goal of this project was to extend high energy kHz repetition rate laser capability to the femtosecond range by using our diode-pumped cryogenic Yb:YAG laser technology to pump a high average power Ti:Sapphire laser. In a milestone achieved during the previous period of performance we generated green pulses ( $\lambda=515$  nm) at a record repetition rate of 1 kHz. A fraction of the power from this new 1 KHz repetition rate green was used to pump the first stage of amplification of the proposed Ti:Sapphire laser system. As part of this project, we demonstrated a room temperature Ti:Sa amplifier that uses a cross pump-seed geometry to generate 30mJ output pulses at 0.5 kHz repetition rate, and 25mJ at 1 kHz when pumped by 100 mJ  $\lambda=515$ nm pump from the diode pumped Yb:YAG laser. The crystal geometry allows to maintain the crystal at  $\sim 30$  C with a water-cooling temperature of 10 C. The amplifier is an attractive solution for use in the first stages of amplification in high peak and high average power chirped pulse amplification laser systems. The results were published in Optics Letters during 2022: V. Chvykov, H. Chi, Y. Wang, K. Dehne, M. Berrill, and J.J. Rocca, "Demonstration of a side-pumped cross-seeded thin-slab pre-amplifier for high-power Ti:Sa laser systems", Optics Letters, 47: 3463, (2022).

## **3. TRAINING OPPORTUNITIES**

The project provided the opportunity to train three graduate students (Han Chi, Kristian Dehne, and Aaron Davenport ) a post-doc, and five undergraduate students. Han Chi graduated with Ph.D in Electrical and Computer Engineering from Colorado State University in August 2021. He is currently employed by KLA (San Jose), a manufacturer of the most advanced tools for the metrology needed by semiconductor industry. Kristian Dehne graduated with an MS in Spring 2023 and is now working in the optics industry in the US.

Dr. Adam Higginson, a post-doc who participated in the project for two years working on laser beam propagation and filamentation experiments , was hired by ASML San Diego where laser-created plasma extreme ultraviolet sources are developed and manufactured to print the most advanced integrated circuits. He joined six Ph. D. graduates from our laser/optics group at CSU who were hired by ASML in the past several years.

Five undergraduate students participated in the project. Two undergraduate students worked on laser development during the summer 2022: Cameron Holmes and Alec Day.



#### 4. TECHNOLOGY TRANSFER

No information to report

#### 5 . PARTICIPANTS

**Principal investigator:** Jorge J. Rocca

**Co-investigator or Co-PI:** Carmen S. Menoni

**Business Contact:** Department of Electrical and Computer Engineering, Colorado State University, Fort Collins, CO 80525

**Other Team Members:** Kristian Dehne (Graduate Student); Han Chi (Ph.D student graduated August 2021); Aaron Davenport (Graduate Student) , Adam Higginson (Postdoc); Yong Wang (Research Scientist), Vladimir Chvykov (Research Scientist), Sina Anaraki Zahedpour (Research Scientist)

None are National Academy Members

**Collaborators:** The measurements of the propagation of high energy picosecond laser pulses in the atmosphere at repetition rates up to 1 kHz were conducted at Colorado State University in collaboration with Prof. Howard Milchberg from the University of Maryland, and his students.

#### 6.STUDENTS

Three graduate students participated in the project during the reporting period: Han Chi (graduated with Ph.D in Electrical and Computer Engineering on August 2021), Kristian Dehne (graduated with a MS, Spring 2023) , and Aaron Davenport. In addition, a post-doctoral student, Adam Higginson, also participated. Five undergraduate students participated in the project.

**Number of students receiving STEM degrees: 2**

Han Chi; Ph.D Degree Summer 2021

Kristian Dehne: MS Degree in Electrical and Computer Engineering Spring 2023

**Number of undergraduate and graduate STEM participants: 5**

5. **PRODUCTS** Publications resulting from this project:

##### **Journal Papers**

1. V. Chvykov, H. Chi, Y. Wang, K. Dehne, M. Berrill, and J.J. Rocca, “Demonstration of a side-pumped cross-seeded thin-slab pre-amplifier for high-power Ti:Sa laser systems”, Optics Letters, **47**: 3463, (2022)

2. A. Higginson, Y. Wang, H. Chi, A. Goffin, I. Larkin, H.M. Milchberg, and J.J. Rocca, Wake dynamics of air filaments generated by high-energy picosecond laser pulses at 1 kHz repetition rate, *Optics Letters*, **46**: 5449, (2021).
3. H. Chi, Y. Wang, A. Davenport, C. S. Menoni, and J. J. Rocca, "Demonstration of a kilowatt average power, 1 J, green laser," *Optics Letters* **45**, 6803, (2020). DOI: 10.1364/OL.412975.
4. H. Wang, A. R. Meadows, E. Jankowska, E. Randel, B. A. Reagan, J. J. Rocca, and C. S. Menoni, "Laser induced damage in coatings for cryogenic Yb:YAG active mirror amplifiers," *Optics Letters*. **45**, 4476, (2020). DOI: 10.1364/OL.399293

### Conference Presentations and Proceedings

1. J.J. Rocca, Y. Wang, K. Dehne, A. Higginson, H. Chi, V. Chvykov, A. Davenport, C.S. Menoni, "Advances in kW average power ultrafast lasers based on cryogenically cooled Yb:YAG lasers and applications," Conference on Ultra-High Intensity Lasers (ICUIL), *ICUIL*, Jeju, South Korea, Sept 18-23, (2022). **Invited**
2. J.J. Rocca, "High Average Power Cryogenic DPSSLs: development and applications" in "XXIII Symposium on High Power Laser Science and Applications", Prague (Prague, June 12-16, 2022). **Keynote speaker**.
3. V. Chvykov, H. Chi, Y. Wang, K. Dehne, M. Berrill, J.J. Rocca, "Cross-Thin-Slab amplifier for high peak power and average power Ti:Sapphire laser systems" Conference on Ultra-High Intensity Lasers (ICUIL), , Jeju, South Korea, Sept 18-23, (2022)
4. V. Chvykov, H. Chi, Y. Wang, K. Dehne, M. Berrill, J.J. Rocca, "Ti:Sa amplifiers for 100s TW laser systems with high repetition rate, Conference on Ultra-High Intensity Lasers (ICUIL), Jeju, South Korea, Sept.18-23, (2022)
5. J.J. Rocca, "High power lasers: from intense x-ray beams to relativistic nanophotonics," **Dvořák Public Lecture**, Institute of Physics of the Czech Academy of Sciences (Prague, June 13, 2022).
6. J.J. Rocca, "New Advances in the Technology and Science of High Power Lasers," in *PQE- (Progress in Quantum Electronics) 2022*, (Snowbird, Utah, 2022). **Plenary Talk**.
7. V. Chvykov, H. Chi, Y. Wang, M. Berrill, and J.J. Rocca, "Demonstration of a Cross-Thin-Slab Amplifier for High Peak and Average Power Ti:Sa Laser Systems" in *Conference on Lasers and Electro-Optics (CLEO)*,: 10.1364/OL.460743 (May, 2022).
8. J.J. Rocca, "KW average power, high pulse energy, ultrafast lasers based on cryo-cooled Yb:YAG," *European Optical Society Annual Meeting (EOSAM) 2021*, (virtual, Italy, 2021).
9. A. Higginson, Y. Wang, H. Chi, A. Goffin, I. Larkin, H.M. Milchberg, and J.J. Rocca, "Wake dynamics of air filaments generated by high energy picosecond laser pulses at 1 kHz repetition rate" in *Annual Meeting of the APS Division of Plasma Physics*, Pittsburgh, PA: APS CP11.00002 (2021).
10. Y. Wang, H. Chi, K. Dehne, C. Baumgarten, A.R. Meadows, A. Davenport, G. Murray, B.A. Reagan, C.S. Menoni, and J.J. Rocca "1 kHz Repetition Rate 1.1 J Picosecond Laser" in *Optica Laser Congress- Advanced Solid-State Lasers 2021*, Washington, D.C.: 10.1364/ASSL.2021.AM2A.4 (2021).

11. J. J. Rocca, "Generation and air propagation of high energy ultrafast laser pulses at 1 kHz" in *2021 Advanced High Power Laser and Beam Control Conference*, virtual: DEPS (2021).
12. J.J. Rocca, Y.Wang, H. Chi, K. Dehne, A. Davenport, C.S., Menoni, "High Repetition Rate, High Pulse Energy, Ultrafast Lasers Based on Yb:YAG", 2021 IEEE Research and Applications of Photonics in Research, August 2-4 , (2021). Virtual conference.
13. Han Chi, Yong Wang, Aaron Devenport, Carmen S .Menoni and Jorge J. Rocca ,," Demonstration of a Kilowatt average power , 1 Joule, green laser", in Conference on Lasers and Electro-Optics (CLEO), 9-14 May (2021)
14. K. Juskevicius, E. Randel, Y. Le, M. Fazio, A. Davenport, C.S. Menoni, "Optical and structural properties of thin film amorphous oxides for photonic structures", 2020 IEEE Photonics Conference. Sept. 29-October 1, (2020). (Virtual Conference).

### **Book Chapter**

1. Jorge .J. Rocca, Yong Wang, Cory Baumgarten, Brendan Reagan, Kristian Dehne, Carmen Menoni, "High Energy, High Power, Ytterbium Lasers" in "Emerging Laser Technologies for High-Power and Ultrafast Science", Editor: Francois Legare, IOP Publishing, Chapter 1, p. 1 (2021).

### **Thesis:**

1. Han Chi, Ph.D, "Development of High-Power, High-Energy Laser System", Colorado State University Electrical and Computer Engineering Department. Summer 2021
2. Kristian Dehne, MS, "Demonstration of Filament Guided Electrical Discharges from a High Average Power 1KHz Laser", , Colorado State University Electrical and Computer Engineering Department. Spring 2021

### **6. Point of Contact in Navy**

Quentin Saulter, ONRA, [quentin.saulter@navy.mil](mailto:quentin.saulter@navy.mil)

Chris Hulse, SETA Support Contractor, [Christopher.a.hulse.ctr@us.navy.mil](mailto:Christopher.a.hulse.ctr@us.navy.mil)

## Appendix A

### Picosecond laser filament-guided electrical discharges in air at 1 kHz repetition rate.

**Abstract:** Laser induced filaments have been shown to reduce the voltage necessary to initiate electric discharges in atmospheric air and guide their propagation over long distances. Here we demonstrate the stable generation of laser filament-guided electric discharge columns in air initiated by high energy (up to 250 mJ) 1030 nm wavelength laser pulses of 7 ps duration at repetition rates up to 1 kHz, and discuss the processes leading to breakdown. A current proportional to the laser pulse energy is observed to arise as soon as the laser pulse arrives, initiating a high impedance phase of the discharge. Full breakdown characterized by impedance collapse occurs 100 ns to a few  $\mu$ s later. A record 4.2-fold reduction in breakdown voltage for dc-biased discharges is observed to be predominantly the result of a single laser pulse that causes a large (>75%) density depression that is practically independent of the repetition rate up to 1 kHz. The radial gaps between the filamentary plasma channel and the electrodes are shown to play a significant role in the breakdown dynamics. A rapid increase of 3-4 orders of magnitude in current is observed to follow the formation of localized radial current channels linking the filament to the electrodes. The increased understanding and control of kHz repetition rate filament-guided discharges can aid their use in applications.

#### 1. Introduction

The propagation of high-power laser pulses in air has been studied since the early years of laser development, motivated by applications. Laser pulses of sufficient intensity led to ionization of air molecules and plasma formation. Beginning in the 1970s, the prospect that this interaction could be used to trigger and guide electrical discharges such as lightning, was experimentally studied with some success [1–3]. Further investigation using high energy laser pulses of long (>100 ns) duration produced high-voltage discharges guided across meter-scale gaps [4–6]. These studies were limited to nanosecond pulse durations, which resulted in the formation of a discontinuous chain of conductive plasma balls. The long pulse duration causes avalanche ionization at the leading edge of the pulse, which produces a dense plasma that is optically opaque to the trailing edge and limits pulse propagation [7]. While guiding was possible due to the conductive plasma balls promoting leader formation [5], the limited pulse propagation and high pulse energy required made these systems poorly suited for guiding discharges over long distances. The development of ultrashort pulse lasers enabled by chirped pulse amplification [8] renewed the interest in this area of research due to their high intensity capabilities. For laser pulses with power greater than the critical power for self-focusing, atmospheric propagation becomes heavily affected by nonlinear responses, resulting in a self-sustaining channeling known as filamentation.

Discovered by Braun et al. (1995) [9], filamentation is primarily the result of a dynamic balance between self-focusing via the optical Kerr effect and plasma defocusing. For femtosecond pulses the result is typically a narrow (of the order of 100  $\mu\text{m}$ ), weakly ionized plasma channel of uniform density, which is capable of propagating tens or hundreds of meters [10] with plasma lifetimes of the order of several nanoseconds [11,12].

Following this discovery, the continuous plasma channel produced by femtosecond filamentation was seen as an effective way to trigger and guide electrical discharges. As with natural lightning, electric discharges in the laboratory are typically initiated through a highly conductive leader which propagates by the formation of streamers at its head. For an atmospheric discharge at sea level, the critical field for spontaneous breakdown is  $\sim 29$  kV/cm. Several experiments were successful in initiating and guiding the discharge process, an effect that was associated with facilitating leader growth between electrodes with the filament formed plasma [13,14]. However, other experiments have shown that discharges triggered and guided by filamentation can also occur in the absence of streamers [15], including those triggered with laser pulse of  $> 2$  ps duration [16]. Due to a relatively low electron density [17] of the filaments generated by mJ-level femtosecond pulses, the generated plasma is weakly conductive [18] and has a short (ns) lifetime, making it poorly suited for sustaining discharges. The hydrodynamic response of the air following filament formation was identified as a mechanism for triggering and guiding discharges [19]. Using time-resolved interferometry [20,21] and diffractometry [22], a low-density channel of similar geometry to the filament was found in the wake of ultrafast pulses. This hydrodynamic response of the air is caused by the deposition of laser energy leading to a pressure wave that expands radially, forming an underdense region [19–23]. This localized depression in air density along the filament path constitutes a channel of lower density that, in accordance with the Paschen curve [24], allows discharges to be initiated by a weaker electric field.

Most laser-guided discharge experiments have been conducted at low repetition rates ( $f = 10$  Hz) with femtosecond lasers [15,25–30]. Ti:Sa based systems have been often utilized due to their capability to produce filamentation with low pulse energy and their widespread commercial availability. Since the localized density depression has been shown to decay by thermal diffusion on a millisecond timescale [21], at such low repetition rates the time between laser pulses allows for complete relaxation of the surrounding air. The more recent development of kHz-level systems capable of generating the high intensity necessary for filamentation has enabled the study of a new regime in which the medium does not completely recover before the arrival of the next discharge-inducing laser pulse. In this regime the effects from pulses in the pulse train accumulate. A few experiments have been conducted with femtosecond Ti:Sa lasers operating at 1 kHz repetition rate [31–33]. They showed the formation of a long-lived, quasi-permanent density depression [31] of greater magnitude than that observed at low repetition rates [32]. This cumulative effect was recently investigated in a study that also reports a reduction in breakdown voltage compared with

low rep rate discharges when voltage is applied by triggering a spark-gap prior to the arrival of a laser pulse [32].

Recently, diode-pumped Yb: YAG-based IR lasers producing high power picosecond pulses at repetition rates at 1 kHz have become available [34–36] for filamentation and discharge guiding research [37–39]. The time between shots at high repetition rates, 1 ms for 1 kHz, allows a given pulse to interact with the air perturbation caused by the preceding pulses [31,37–39]. Filament lengths up to 70 m have been recently reported with 720 mJ laser energies and pulse durations of 0.92 ps at 1 kHz [40]. One such laser system has recently successfully guided a lightning discharge over a distance of 50 m [41]. Results of breakdown voltage for single shot near-infrared laser pulses of up to 10 J energy and durations between 0.7 and 10 ps found a further 30% reduction for the longer pulses [16]. In an experiment conducted with 1030 nm 0.9 ps laser pulses of 150 mJ energy at 1 kHz repetition rate a reduction in breakdown voltage by a factor of more than 2 X was reported [37]. A study with 1030 nm, 1.5 ps pulses of 100 mJ energy found a factor of 3 X reduction in breakdown voltage when the repetition rate was increased from 10 Hz to 1 kHz [38]. This breakdown voltage reduction was attributed to the cumulative effect of the hydrodynamic response of the air around the filament at high repetition rates.

Here we examine discharges guided by the filamentation of high-energy picosecond pulses of 7 ps duration and up to 250 mJ energy from a  $\lambda_L = 1030$  nm wavelength laser operating at repetition rates of up to 1 kHz. We demonstrate the repetitive generation of stable discharge columns at this repetition rate. A record breakdown voltage reduction of up to 4.2 X for gaps of up to 10 cm between cylindrical electrode plates with an axial hole is observed to result predominantly from the perturbation caused by a single laser pulse, leading to measured density depressions reaching  $>75\%$ . The breakdown voltage reduction is observed to be similar at 100 Hz and 1 kHz repetition rate. A current proportional to the laser pulse energy arises as soon as the laser pulse arrives, initiating a high impedance discharge. Full breakdown, characterized by impedance collapse and the onset of high current conduction, occurs 100s of ns to a few  $\mu$ s latter, following the formation of concentrated conducting channels in the radial gaps between the filamentary plasma channel and the electrodes. The experimental evidence shows that the role of these gaps, often neglected, needs to be considered in analyzing the breakdown dynamics of short distance laser-filament guided discharges.

## 2. Experimental set up and methodology

The experiments were performed using a  $\lambda_L = 1030$  nm wavelength laser pulses of 7 ps duration from a cryogenically cooled, diode-pumped chirped pulse amplification Yb: YAG laser system developed at Colorado State University that operates at repetition rates up to 1 kHz [34]. A schematic of the experimental setup is shown in Fig. 1. After compression, a 3-cm-diameter S-

polarized beam is focused to a  $\sim 70 \mu\text{m}$  (FWHM)-diameter spot using a 2.2 m focal length lens. The repetition rate ( $f$ ) of the laser pulses was varied between  $f = 0.01$  to 1 kHz, and the laser pulse energy ( $E_L$ ) was varied in the range  $E_L = 10 - 250$  mJ by selecting the energy of the seed pulse injected into the cryo-cooled power laser amplifiers. The pump pulse energy to the power amplifiers was maintained constant to avoid significant variation in the thermal lens. The electric discharge electrodes are two circular parallel brass plates with a face diameter of 13 cm, which are curved around the edges to increase field uniformity. Holes of 3.8 mm diameter were drilled on axis to allow the laser beam to pass through. The separation of the two plates varied in the range  $d = 2$  cm to 10 cm. A 1.7 nF ceramic capacitor was directly connected to the anode electrode and the cathode was grounded. The capacitor was charged using either a current supply (Glassman PS/LT015P132) or a voltage supply (Hipotronics 8100-10), operated at up to 15 kV or 50 kV, respectively. The output of the current supply is more highly filtered, offering a more stable source for repetition-rated discharges, while the voltage supply, which can provide a higher output voltage, was used for larger electrode separation measurements. The charging resistor was selected to be either  $R_c = 280 \text{ k}\Omega$  or  $R_c = 175 \text{ M}\Omega$ . The lower value was used for faster charging of the capacitor in the high repetition rate measurements, such that the capacitor is nearly fully charged when the next laser pulse arrives. The higher resistor value was used for breakdown measurements at lower repetition rate, for which the train of laser pulses samples the gap for breakdown as the voltage slowly increases. Figure 1(a) shows a photograph of a typical laser filament, and Fig. 1(b) shows a 10-cm-long laser-guided discharge channel integrated over 17 discharge events at 1 kHz repetition rate. A well-behaved straight channel is observed.

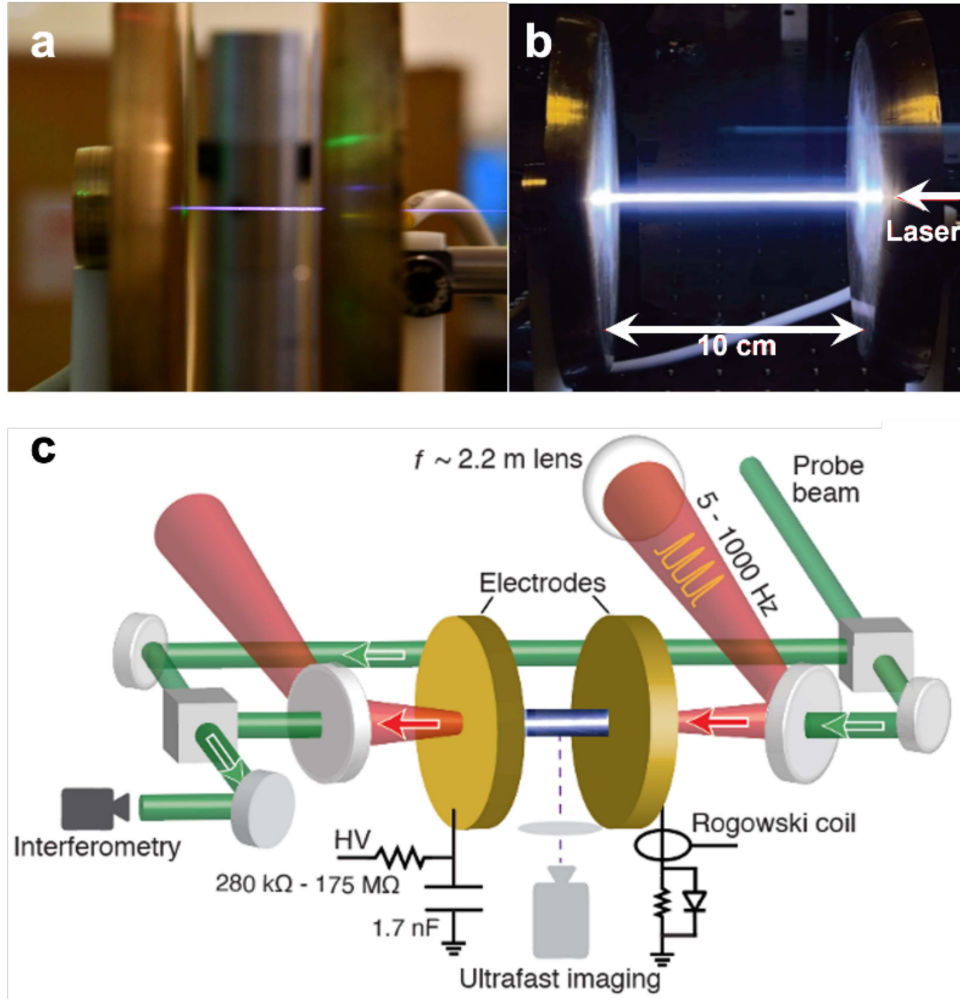


Fig. 1. (a) Laser filament generated at 1 kHz. (b) Photograph integrated over 17 discharge events, taken with a 60 frames per second camera for a laser pulse energy of 200 mJ, repetition rate 1 kHz, and plate separation of 10 cm. (c) Schematic of the experiment set-up. The probe beam is shown in the longitudinal configuration. The charging resistance ( $R_c$ ) varies in the range  $R_c = 280 \text{ k}\Omega - 175 \text{ M}\Omega$ . The power supply ( $HV$ ) is either a voltage or current supply, as detailed in the main text. The current pulse is monitored with a Rogowski coil placed in the ground loop or alternatively by measuring the voltage drop in a shunt resistor.

A combination of optical and electrical diagnostics was implemented to characterize the discharges over a wide range of conditions. The electrical diagnostics consisted of a high voltage probe to measure the breakdown voltage, and a magnetic probe to measure the current pulse. The voltage drop across a resistor placed in the ground electrode connection was measured with a differential probe to provide an additional measurement of the current. Photodiodes were used to measure the timing of the filament-creating laser pulse and optical probe pulse arrival with respect to the discharge event. These diagnostics were coupled to a deep-memory digital oscilloscope with 3 GHz analog bandwidth (LeCroy Wavepro 7300A), capable of acquiring traces with duration of



seconds with 10 ns temporal resolution. Several optical diagnostics were fielded. An imaging system measured the discharge-generated light, recording either time-integrated or time-resolved image sequences. The latter made use of a fast micro-channel plate intensified framing camera (Invisible Vision Ultra UHSi-12) capable of recording up to 12 frames of variable temporal separation with a minimum exposure window of 5 ns. Its sequential gating capability allowed to monitor the early formation of the discharge by recording sequences of images of the discharge channel fluorescence with this time resolution. Mach Zehnder interferometers using a second harmonic green probe beam were deployed in three different angular configurations: longitudinally along the discharge axis (case illustrated in Fig 1 (c)), transversely at a grazing incidence angle of 11.5 degrees, or at normal incidence to probe the discharge channel evolution. Time-resolved interferograms were recorded using either the gating provided by the second harmonic probe laser pulse ( $\sim 5$  ns resolution) and a standard CCD camera, or the high-speed gating camera (also 5 ns image resolution).

## 2. Results and discussion

### 2.1 Discharges at 1 kHz

Figure 2 shows an example of electrical data for a train of laser filament- guided discharges at 1 kHz repetition rate. Displayed are the laser pulse time-of-arrival measured with a photodiode (a), the current pulse (b), and the voltage drop across the gap (c) for approximately 100 consecutive discharges. The electrode gap was  $L=2$  cm, and the laser pulse energy was  $E_L = 150$  mJ. The voltage of the current supply was set to 15 kV to charge the capacitor through a  $R_c = 280$  k $\Omega$  resistor, corresponding to a charging time constant of  $\tau = 0.5$  ms. The time interval between laser pulses is 1 ms, meaning that at the time the subsequent laser pulse arrives the capacitor is charged to about 86% of its maximum voltage, sufficient to consistently initiate a discharge event upon the arrival of each laser pulse. Notice in Fig. 1c that the current of the initial discharge of the sequence, which corresponds to having the capacitor fully charge and suddenly unblocking the laser beam, is larger due to the larger initial overvoltage respect to the reduced breakdown voltage observed in later pulses. Figure 2(b) shows that each subsequent laser pulse triggers a breakdown event with highly reproducible current pulses. The average power dumped into the discharge at the conditions of Fig.2 is  $\sim 150$  W. Figure 2(d) displays a zoomed-in image of a typical set of current and voltage measurements for a single discharge event. The current is underdamped (Fig. 2d). The time of laser pulse arrival is indicated.

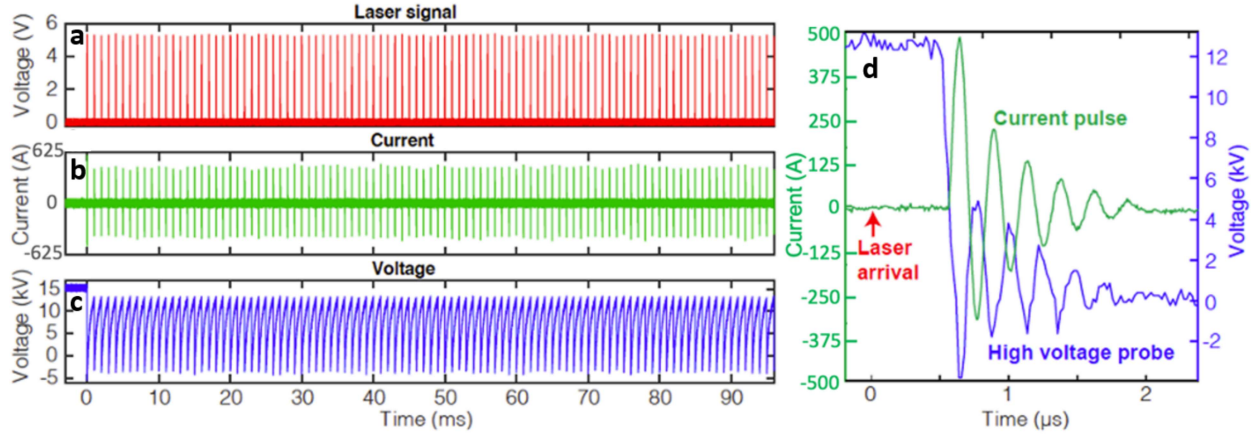


Fig. 2. (a-c) Electrical measurements (labelled) of a laser-guided discharge operating at a repetition rate  $f = 1.0$  kHz, with laser energy  $E_L = 150$  mJ and electrode separation  $d = 2$  cm. A sequence of approximately 100 laser-triggered discharges is shown. (d) Example single discharge event.

In general terms the action of the laser pulse is twofold: it reduces the breakdown voltage ( $V_b$ ) required to initiate a discharge event and provides a straight channel for the current to flow. To accurately determine  $V_b(E_L, L, f)$ , the capacitor was charged slowly with  $R_c = 175$  M $\Omega$  (corresponding to  $\tau = 300$  ms) and the laser was left unblocked while operating at 1 kHz repetition rate, or at an alternatively chosen repetition rate. In this way the high repetition rate pulse train samples the constantly increasing voltage until breakdown is achieved. In the absence of a laser pulse, the breakdown voltage is expected to follow the typical behavior of a high voltage air gap. The breakdown voltage dependence on gas density and other characteristics of electrical breakdown in gases have been thoroughly studied for many years, in particular in connection with spark gaps and pulsed-power switching [42–45]. The relationship between air density and breakdown electric field for gaps of sufficient length is described by the well proven relationship [46,47]:

$$V_b(\text{kV}) = 24.4\rho d(\text{cm}) + 6.5\sqrt{\rho d(\text{cm})}, \quad (1)$$

where  $V_b$  is the breakdown voltage,  $d$  is electrode plate separation, and  $\rho$  is the air density relative to its value at a pressure of 1 atm for a temperature of 20 C. During our experiments, the air pressure and temperature were measured to be 0.84 atm and 25 C, respectively, which corresponds to  $\rho = 0.83$ .

Figure 3(a-d) displays  $V_b$  as a function of laser pulse energy  $E_L$ , for four different discharge gap distances  $d = 2, 4, 8$ , and 10 cm and two different repetition rates,  $f = 100$  Hz and 1000 Hz. To be able to apply a sufficiently high voltage to achieve breakdown in the longest gaps, the current supply (limited to 15 kV) was substituted by the voltage supply with higher output voltage capability. The measured (or extrapolated) breakdown voltage in the absence of a laser pulse is indicated in black. For  $d = (0.5, 1, 1.5$  and 2 cm), the breakdown voltage  $V_b(E_L = 0$  mJ) was observed to agree well with the expected dependence as a function of inter-electrode distance given

by Eq. (1) (Fig. 3(e, f)). A linear best fit to the data is shown as a dashed line for the laser-initiated discharges.

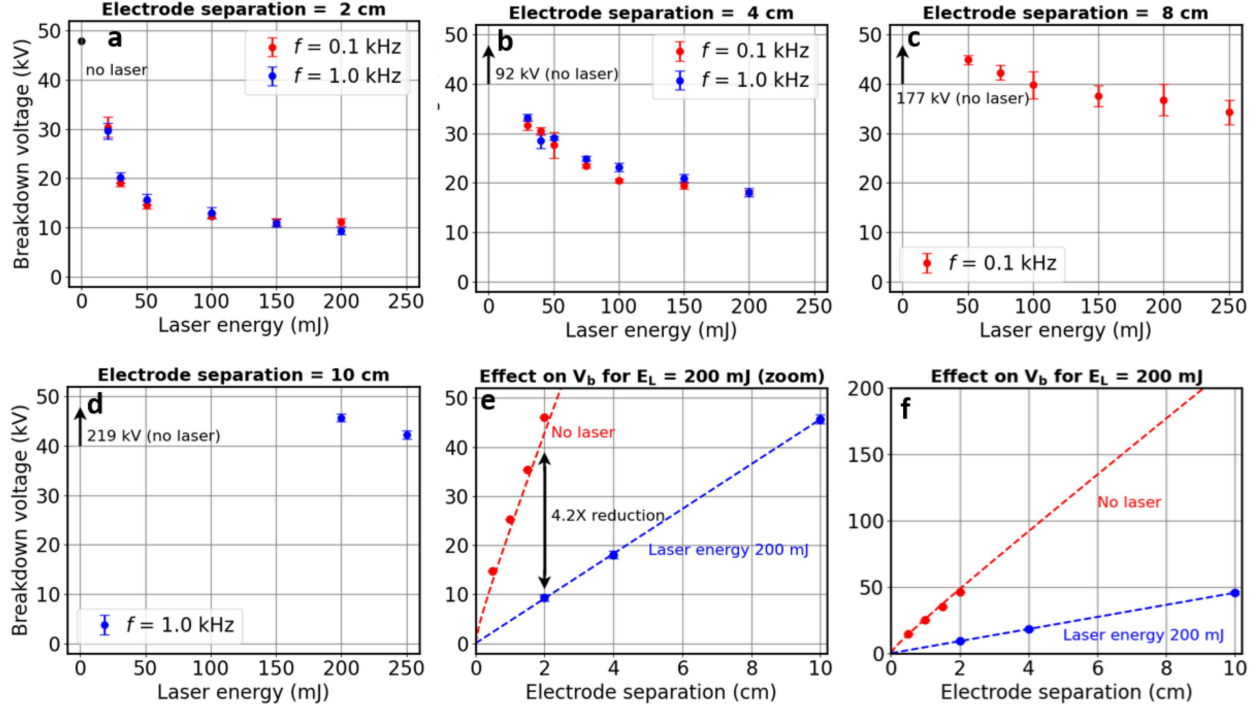


Fig. 3. (a-d) Breakdown voltage ( $V_b$ ) as a function of laser pulse energy ( $E_L$ ), for two laser pulse repetition rates (0.1 and 1 kHz) and four electrode separations (a)  $d = 2$  cm; (b)  $d = 4$  cm; (c)  $d = 8$  cm and (d)  $d = 10$  cm. The breakdown voltage without a laser pulse ( $E_L = 0$ ) indicated for the longer discharges is calculated using Eq. (1). (e-f)  $V_b$  as a function of  $d$ , for  $E_L = 200$  mJ alongside the no-laser case. (e) Zoomed-in voltage axis; (f) full voltage axis. For the no-laser data, the dashed line corresponds to Eq. (1). For the laser-initiated discharges the dashed line corresponds to a linear fit to the measured data.

Figure 4 (a) and (b) show the breakdown delay, defined as the time between the arrival of the laser pulse and the breakdown, as a function of applied voltage and laser pulse energy. The data here corresponds to a 2-cm-long discharge at 5 Hz repetition rate. The breakdown delay time and the jitter both decrease as the applied voltage is increased and as the laser pulse energy increases. However, for voltages larger than 20 kV no significant further decrease in breakdown delay is observed when the laser pulse energy is increased above 100 mJ. With 100 mJ applied the breakdown delay decreases from 1  $\mu$ s when 15 kV is applied to 30 ns for 40 kV.

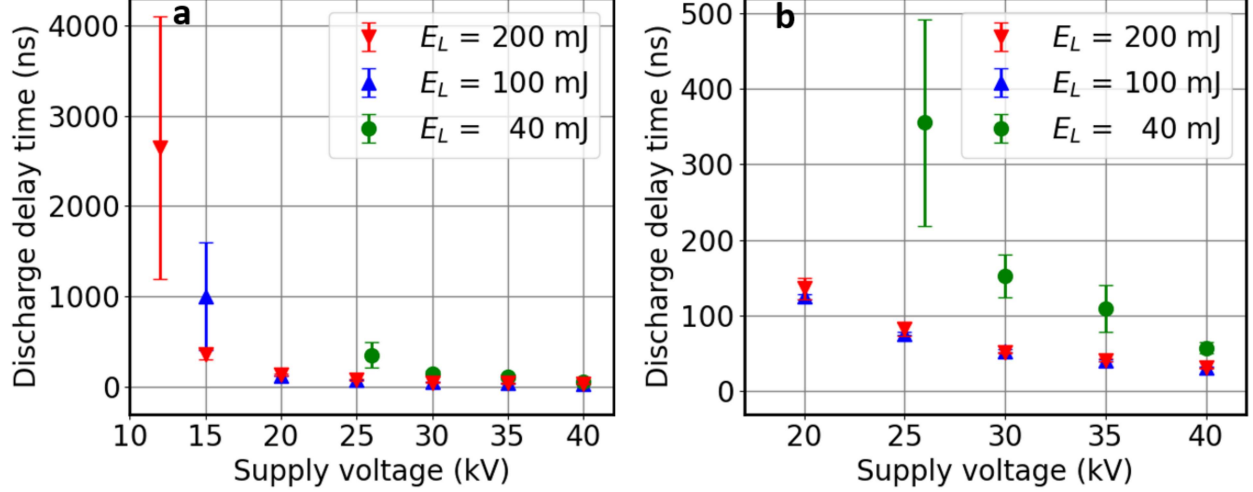


Fig. 4. Discharge breakdown delay as a function of applied voltage for discharges initiated by laser pulses with three different energies. The electrode gap was 2 cm. A zoom of the data in a) for delays less than 500 ns is illustrated in b) for better visualization. For voltages above 25 kV no further reduction in breakdown delay is observed for laser pulse energies greater than 100 mJ.

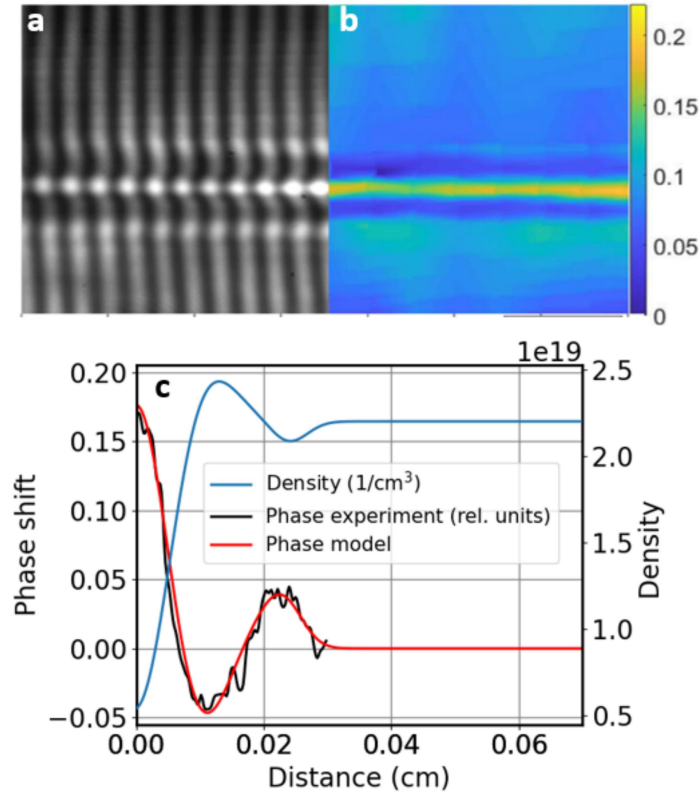
## 2.2 Breakdown Voltage Reduction.

A reduction in breakdown voltage  $V_b$  of up to 4.2 X was measured when a sufficiently high laser pulse energy is used, as shown in Fig. 3. The laser pulse energy has a clear effect on  $V_b$ . For  $d = 2$  cm, Fig. 3(a) shows a sharp drop in  $V_b$  as the laser pulse energy  $E_L$  is increased from  $E_L = 0$  mJ to 50 mJ. For  $E_L > 50$  mJ, the effect of increasing  $E_L$  become less pronounced, with  $V_b$  finally reaching a plateau. Figure 3(e, f) show that for  $E_L = 200$  mJ, the breakdown voltage is reduced by a factor between 4-4.2 X over the entire range of interelectrode distance investigated when compared to the no laser case.

Figure 3(a, b) also shows that the breakdown voltage is practically the same at  $f = 1$  kHz and  $f = 100$  Hz. This indicates that the repetition rate plays no major role in the value of  $V_b$ , implying that the large measure reduction in  $V_b$  is mostly a single-pulse phenomenon instead of the result of the cumulative pulse effects that occur at high repetition rate. Previous studies of laser filaments generated at high repetition rate have reported the creation of a permanent density depression resulting from the cumulative effect of multiple shots [21,32]. In a previous experiment conducted with the same laser, a density depression of  $\sim 20\%$  induced by the previous pulses was measured 10  $\mu$ s before the arrival of a laser pulse in a 1 kHz pulse train [39]. It has been suggested that such lower density channel can reduce the breakdown voltage and guide electrical discharges by producing a preferential channel for the current to flow [21,32,38]. In the experiments described herein it was observed that the reduction in breakdown voltage far exceeds the value that can be attributed to the existence of the measured 20% pre-formed air density depression. Equation (1) indicates that a 20 percent density reduction for  $d = 2$  cm and  $d = 4$  cm should lead to  $V_b$  reductions of 18.4 and 18.8 percent, respectively. In contrast, the maximum  $V_b$  reduction we measured

exceeds 75%. The same expression predicts that the relative density required for such voltage reduction should be  $\rho \sim 0.19$ , corresponding to a density reduction of 78% with respect to the atmospheric pressure during the experiment. In agreement with this expectation, the density depression measured with grazing incidence interferometry shortly after the arrival of a laser pulse approaches this value. Fig. 5(a,b) shows an interferogram corresponding to the channel formed 300 ns after the arrival of a 200 mJ laser pulse and the corresponding phase-shift map. Fig. 5(c) shows the corresponding density profile obtained assuming cylindrical symmetry, which indicates that at this time the density depression reaches  $\sim 75\%$ .

Fig. 5. Grazing incidence interferograms acquired 300 ns after the arrival of a 200 mJ laser pulse. The phase shift (b), and density profiles (c) are shown. The air density depression on axis reaches



75%.

The evolution of the laser-generated channel was modeled with the hydrodynamic code RADEX using as initial electron temperature of 2.5 eV estimated with a particle-in-cell simulation and an initial column diameter of 60  $\mu\text{m}$  [48]. The hydrodynamic simulations results are found to be relatively insensitive to the initial electron temperature between 2 and 5 eV. Electron thermalization occurs in picoseconds due to collisions with neutral and ionized species. Fig.6 shows the computed radial density distribution as a function of time referenced to the arrival of the laser pulse. The air density depression reaches 82 % at  $\sim 100$  ns after the arrival of the laser pulse, and remains at practically the same value for at least several  $\mu\text{s}$ . This is in good agreement with the interferometrically measured values, as illustrated in Fig.7 illustrates the measured density

profiles for three different times in the channel evolution. Both show similar channel depth and widths, and speed of propagation of the shockwave. The profile of the latter is, however, smoother in the experimental plot. This can be expected as it is an average of different regions of the channels which might not to be perfectly uniform.

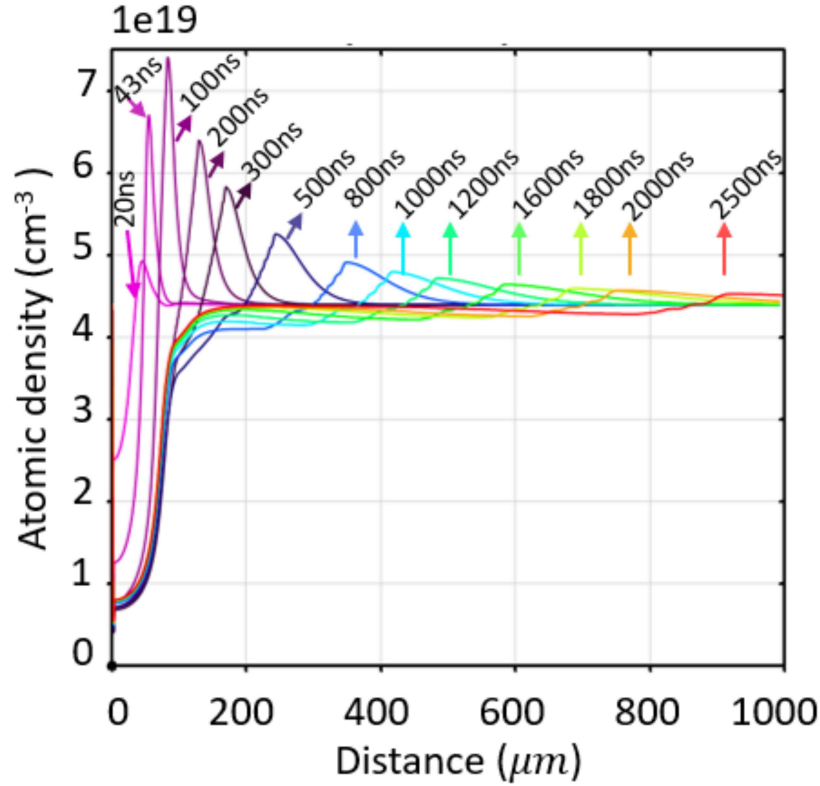


Fig.6. Computed density profile of channel generated by a 150 mJ laser pulse. A density depression of  $\sim 82\%$  develops  $\sim 100$  ns after the arrival of the laser pulse.

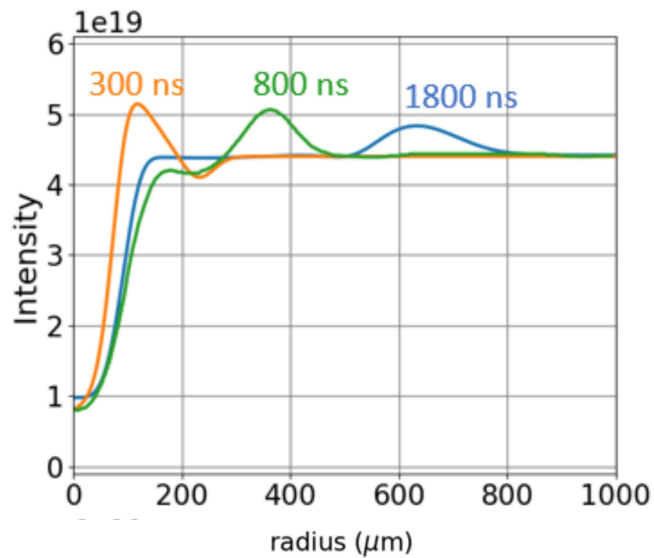


Fig. 7. Interferometrically measured density profile for three times of the channel evolution.

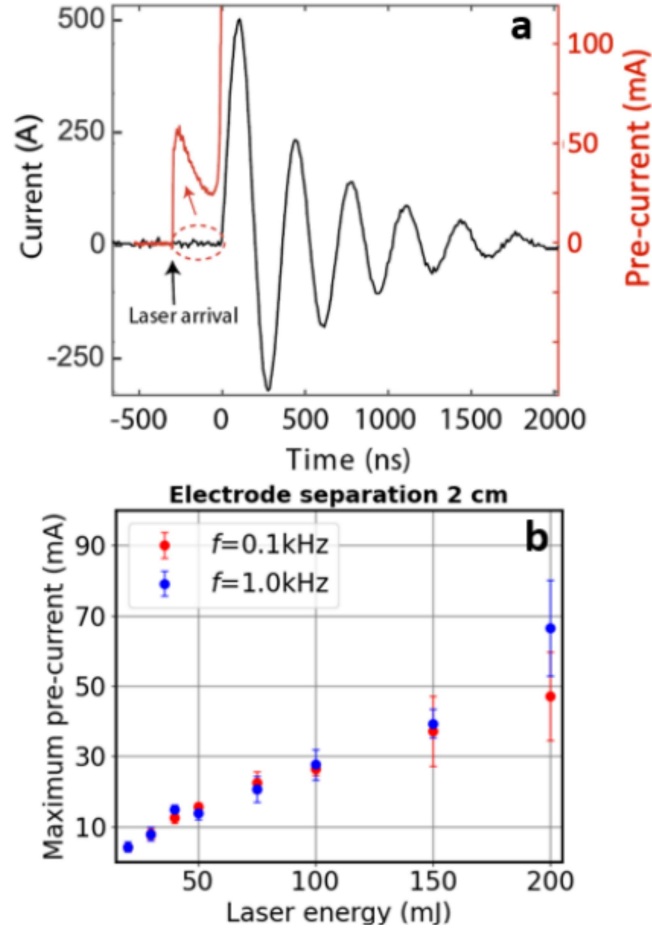
In conclusion, the above measurements and simulations indicates that the large density depression (75-80%) that follows a single laser pulse, possibly combined with the mildly ionized conductive channel that is created with the aid of the detected pre-breakdown current discussed below, is the dominant factor in decreasing the breakdown voltage. Supporting this conclusion is the fact that  $V_b$  for 100 Hz and 1000 Hz laser filament-induced discharges was measured to be practically the same, as illustrated by the measurements in Fig.3 (a, b). This independence of the breakdown voltage with repetition rate differs from the results of an experiment that reported a reduction of the breakdown voltage at increased repetition rate [38]. However, another experiment performed with the same set up that incorporates a triggered spark-gap in series, observed similar breakdown voltages at 10 Hz and 1kHz when voltage was applied at the time of the laser pulse ( $t=0$  in Fig. 2a of Ref. 32), in agreement with our measurements. In any case, it should be noticed that if voltage were to be suddenly applied long after the arrival of a laser pulse, the deeper air cumulative depression present at high (e.g., 1 kHz) repetition rate would result in a lower breakdown voltage, as has been reported in the literature [32]. One should therefore separate the effect of repetition rate on lowering breakdown voltage into the two cases.

### 2.3 *Initial current flow and breakdown*

We now turn our attention to the process leading to full breakdown. In our experiment a static electric field is established between the electrodes before the arrival of a laser pulse. The laser pulse generates a filament which length extends beyond the electrodes. Initially optical field ionization strips electrons from the molecules creating a heated plasma channel that generates a radially expanding shockwave and an air density depression. In the case of the 7 ps duration laser pulses used in these experiments avalanche ionization is the dominant ionization mechanism [39]. A current flow is observed to arise immediately after the arrival of the laser pulse with typically several tens of mA, but that can reach values up to 400 mA. This initial current takes place during an initial high impedance phase of the discharge that precedes the time of full breakdown characterized by the collapse of the impedance. A previous experiment with a short laser filament driven spark gap identified the formation of a field-driven current ( $< 0.15 \mu\text{A}$ ) that was reported to contribute to both deepening the channel and increasing its conductivity by resistive heating, leading to eventual breakdown [21]. In our case the amplitude the pre-breakdown current is typically three to four orders of magnitude smaller than the current after breakdown. Its onset is characterized by a rapid rise that is likely to be associated with a displacement current caused by the re-arrangement of charges generated by the laser pulse in the applied electric field. This initial current rise is followed by a sustained current whose magnitude and temporal evolution depend on the laser pulse energy and the applied electric field. Figure 8a illustrates the pre-current pulse for the case of a 2-cm-long discharge with an applied voltage of 15 kV initiated by a 150 mJ. Fig. 8 (b) illustrates how the pre-current magnitude increases as a function of laser pulse energy from 15 mJ to 200 mJ, in the case of a 2 cm electrode gap biased at 20 kV. The pre-current magnitude is



similar at 100 Hz and 1000 Hz, and also for discharges of 2 cm and 4 cm length when the same electric field is applied across the electrodes. Following its initial fast rise, the evolution of the pre-current can vary, stabilizing or even decreasing in magnitude before the breakdown occurs. These scenarios have been previously observed in spark discharges in air at atmospheric pressure. This includes cases in which the initial current spike is followed by a transition phase during which



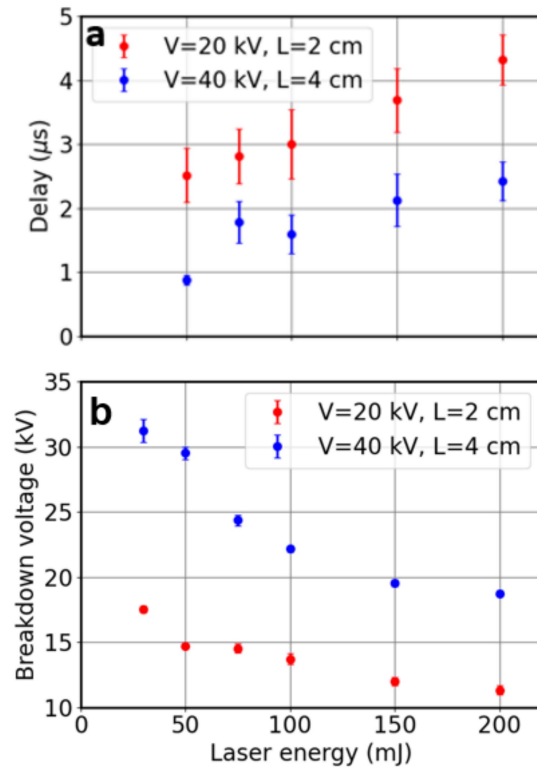
electron attachment to oxygen temporarily prevents the full breakdown [47,49].

Fig.8. a) Current evolution illustrating the pre-breakdown current initiated with a 150 mJ laser pulse in a 2 cm discharge gap biased at 15 kV. b) pre-breakdown current as a function of laser pulse energy for discharges at 100 Hz and 1 kHz repetition rate.

The typical value of the impedance in this pre-breakdown phase ranges from 0.2 M $\Omega$  to a few M $\Omega$ , depending on laser pulse energy and the voltage applied. The discharge impedance is the sum of the resistance of the filamentary axial plasma column between the electrodes, and the resistance of the radial gaps between the column and the electrodes. The non-negligible role of these gaps becomes evident by conducting measurements in discharges with similar electric field/molecular density ratio ( $E/N$ ), a scaling parameter in electrical discharges. For this purpose, we conducted measurements comparing discharges across 2 cm and 4 cm electrode spacing applying twice the



voltage in the 4 cm case. The measured breakdown voltage was found to nearly double in the case of the longer channel, as shown in Fig. 9a. However, the time delay between the arrival of the laser pulse and the breakdown was measured to significantly decrease in the case of the 4 cm discharge (Fig. 9b). This can be ascribed to the fact that in this case the gaps between the filament-initiated plasma column and the electrodes are subject to twice the electric field. This indicates that the role of these small gaps ( $<1.9$  mm between the filament channel and the electrode) in the breakdown cannot be neglected.



**Fig.9.** Breakdown voltage (a), and breakdown delay respect to the arrival of the laser pulse as a function of laser pulse energy (b) for 2 cm and 4 cm electrode separation. The voltage applied was adjusted to have initially equal  $E/N$  values.

On-axis interferograms acquired at different times of the plasma evolution shown in Fig. 10 give additional information on the transition from the high impedance phase into the high current phase following breakdown. Interferograms taken early during the pre-breakdown current-conducting phase do not identify a concentrated current path across the gaps between the filament and the electrodes (Fig. 10a). It is possible that during this high impedance discharge phase the current is conducted across the gap by a high-impedance, spatially distributed glow-type discharge. Glow discharges are known to take place in air at atmospheric pressure and have been the subject of several studies [50,51]. The regions near the electrodes in glow discharges are locations with high electric field and therefore the cradle of instabilities which lead to constriction and arc formation. These discharges are known to undergo glow-to-arc transitions [51] in which the glow plasma collapses into an arc. These glow-to-arc transitions are accompanied by a collapse of the

impedance. Fig. 10 (b)-(d) reveal the formation of concentrated discharge channels in the gap between the filament-initiated discharge column and the electrodes. This occurs a hundred ns to several  $\mu$ s after the arrival of the laser pulse. Two radial arcs are observed to form, each linking the filamentary column to one of the electrodes. Once these concentrated radially conductive channels are formed across the gaps, the collapse of the impedance leads to the rapid increase of the current which rapidly heats the plasma in these channels, causing them to expand at a higher rate [Fig. 10 (c), (d)]. At this stage the capacitor, which voltage drops only very slightly during the pre-breakdown phase, is rapidly discharged.

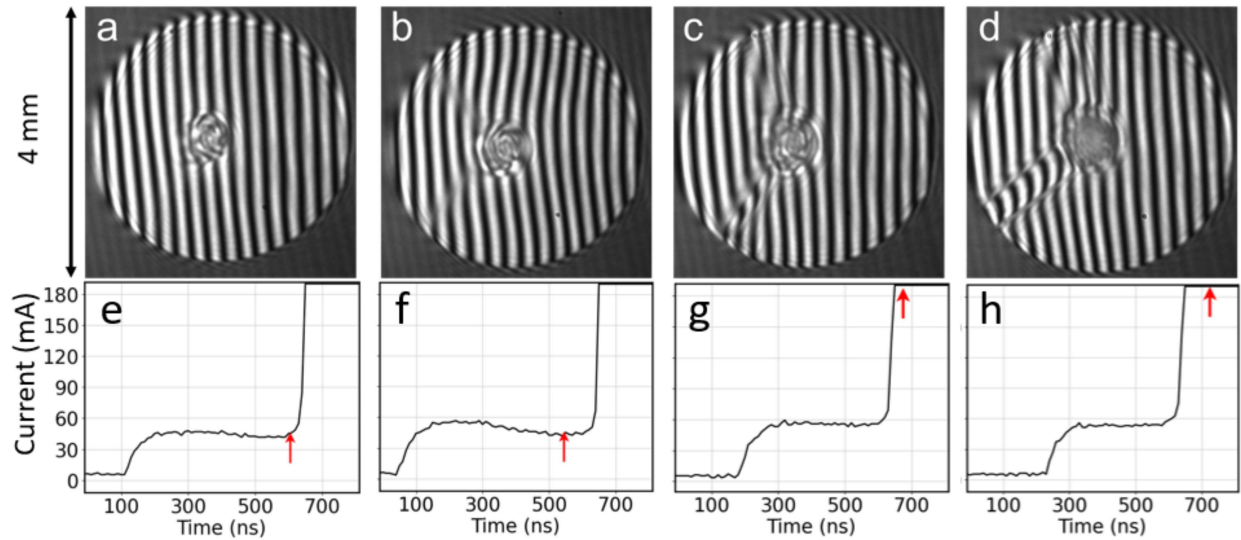


Fig. 10. a-d) On-axis interferograms showing the development of plasma channels linking the laser filament-initiated plasma column to the hollowed electrodes. The region with fringes corresponds to the electrode hole diameter of 3.8mm e-g) Current pulses indicating the time at which the data corresponding to each frame was taken (arrow). The data corresponds to an electrode distance of 2 cm and laser pulse energy of 136 mJ for a pulse train at 100Hz. The region with fringes corresponds to the electrode hole diameter of 3.8mm.

### 3.4. Onset and evolution of the high current discharge channel.

The evolution of the plasma column immediately before and after the time of breakdown was observed using fast sequential imaging with a temporal resolution of 5 ns. Figure 11 shows the first five frames of a sequence of 12 contiguous 5-ns resolution images mapping the evolution of the discharge during the first 60 ns after breakdown. The electrode gap is 4 cm in length. Prior to breakdown no light is detected by the MCP-intensified camera. When plasma light emission is first detected in the first 5 ns frame after breakdown, is observed to be uniform across the entire gap. It is observed to grow in intensity on every frame thereafter as the current increases. No evidence of streamers propagating across the electrode gap is detected. At a velocity of  $1 \times 10^8$  cm/s, on the high end of the typical velocity for streamers, it would take 40 ns for a streamer to bridge the electrode gap, a sufficiently long time for the framing camera to detect it.

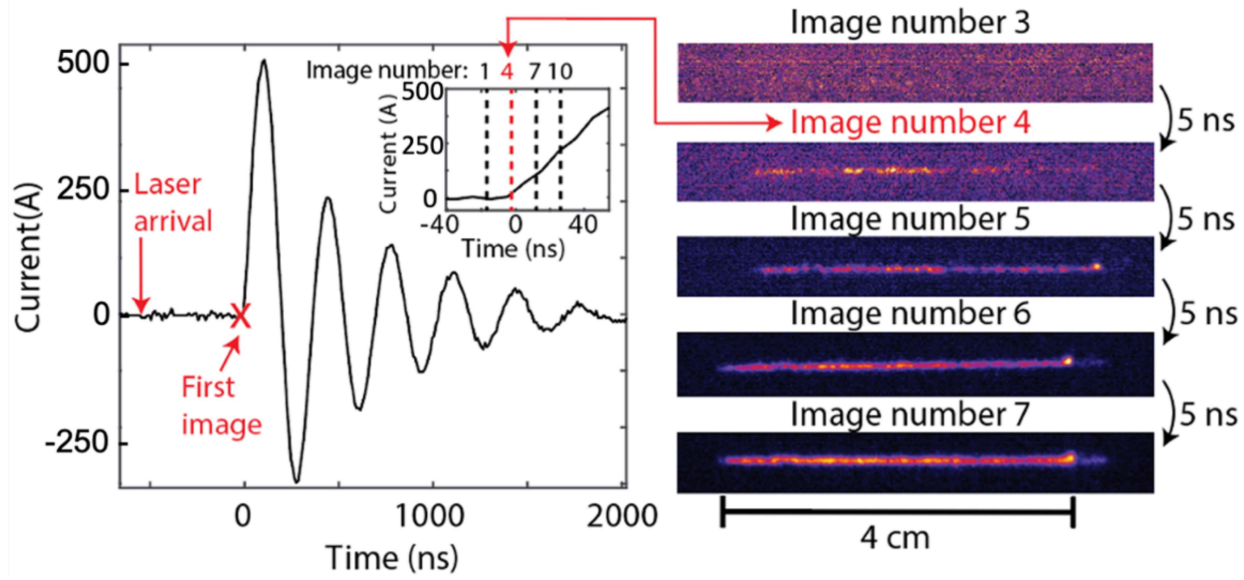


Fig. 11. Sequence of images of the plasma column near the time of breakdown taken 5 ns apart. The time of each image respect to the current pulse is indicated.

Interferograms acquired at different times during the low current phase that precedes the breakdown also show a uniform channel bridging the electrode gap, providing additional evidence suggesting that the filamentary charge created by the laser pulse starts to flow uniformly across the gap, without evidence of streamers. As mentioned above other streamless laser-filament initiated discharges have been previously reported [15,16].

On axis interferograms/shadowgraphs were used to quantify the propagation of the shockwave and discharge channel expansion. Fig. 12 shows a sequence of on axis interferograms corresponding to 100 Hz and 1kHz discharges. A shockwave is observed to propagate outwards at a velocity of  $\sim 350$  m/s, in agreement with the simulation in Fig.6. Absorption of the probe beam along the column creates a darkened region without fringes that grows with time. This dark area is associated with the channel but has a more complex nature, as it depends not only on density but also on temperature, charge, and propagation of light in the channel. Figure 13 illustrates the growth of this region as a function of time for the case of a filament generated by a 150 mJ laser pulse. When the discharge is present, the current that flows in the high impedance phase of the discharge contributes to increasing the expansion [red markers in Fig. 13 (b)], in agreement with the role of this pre-current reported in Ref. 22. After the breakdown occurs, the rapid current increase results in greatly enhanced ohmic heating that leads to a rapid increase in the channel expansion rate reaching velocities of  $\sim 2400$  m/s. In the example of Fig. 13 the channel is observed to expand more than 0.3 mm in 100 ns.

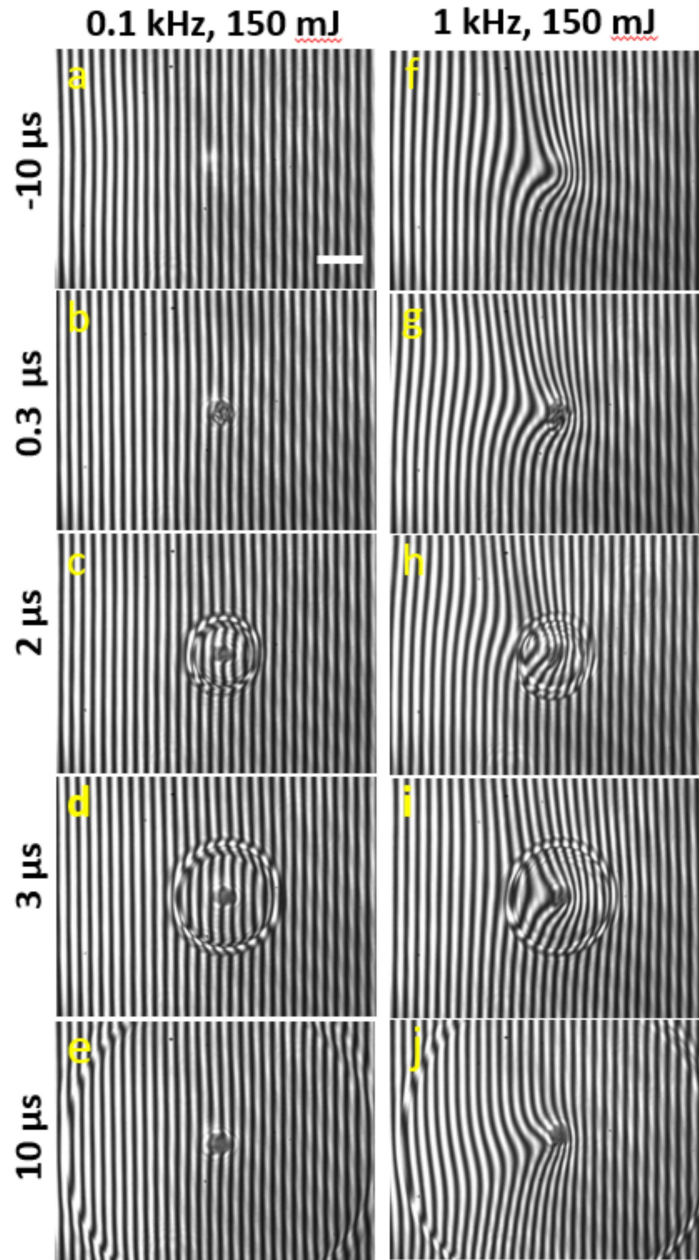


Fig. 12. Permanent density depression at high repetition rate and shockwave formation. Longitudinal interferograms for  $E_L = 150\text{mJ}$  at  $f = 100\text{ Hz}$  (a-e) and  $f = 1\text{ kHz}$  (f-j). Times are indicated with respect to the arrival of the laser pulse. A noticeable perturbation is present  $10\text{ }\mu\text{s}$  prior to arrival of the laser pulse at  $1\text{ kHz}$  (f), and persists. No such perturbation exists for  $100\text{ Hz}$  (a-e). Scale bar is  $1\text{ mm}$ .

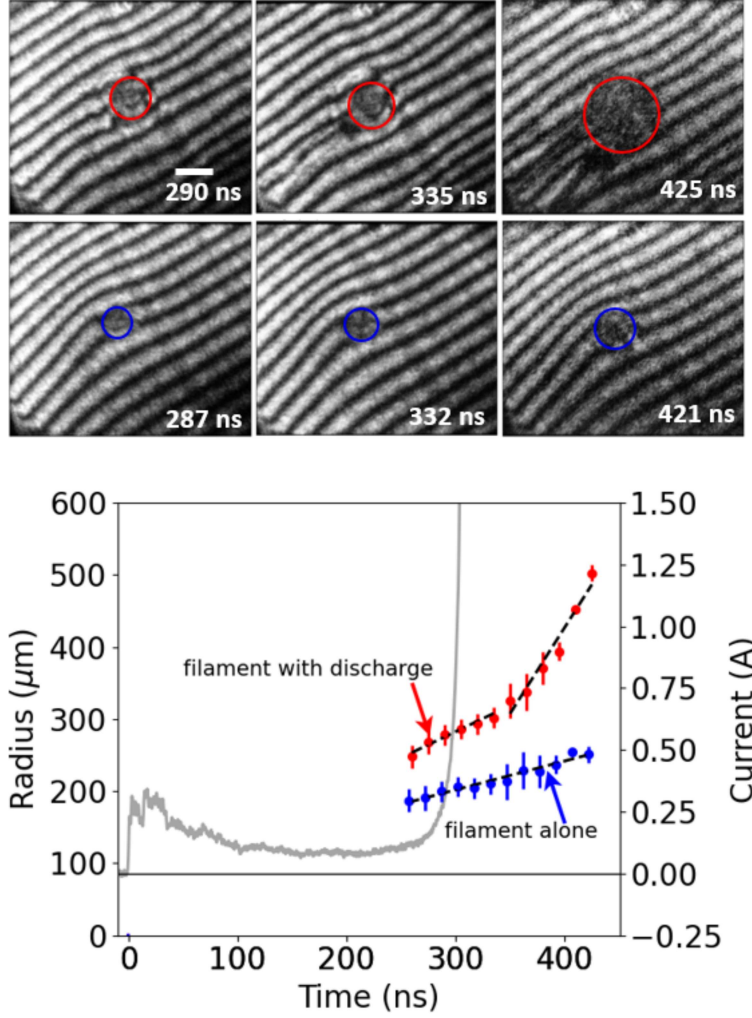


Fig. 13. (a) Interferograms obtained for the filament with voltage applied (upper images) and filament alone (bottom images), for a discharge initiated by 1kHz, 150 mJ laser pulses. The labels indicate the delays. (b) Evolution of the dark region radius before and after breakdown for the case of a laser filament alone (no voltage applied) and a filament with voltage applied. A rapid increase is observed to occur after breakdown. The current pulse is shown as reference (gray line). Scale bar is 500  $\mu\text{m}$ .

### 3.4 Conclusions

We have used laser filaments generated by  $\lambda_L = 1030$  nm, 7-ps long pulses of up to 250 mJ energy to initiate and guide atmospheric stable electrical discharges at repetition rates of up to 1 kHz. The laser-created filament is shown to reduce the discharge breakdown voltage by a factor of up to 4.2 X, which is to our knowledge the largest reported reduction for a discharge between dc biased electrodes. The laser pulse arrival and filament formation are observed to cause the immediate onset of current flow between the biased electrodes, which magnitude of typically several tens of mA is proportional to the laser pulse energy. This phase in the discharge evolution precedes the full breakdown and is characterized by an impedance in the range of 0.2 MOhm to a few MOhm. The gaps between the filament and the discharge electrodes are observed to play a significant role



in the breakdown dynamics. Axial interferograms taken during this pre-breakdown phase show the absence of concentrated current flow between the filament and the electrodes. This suggests that during this initial phase the current across these gaps is conducted by a diffuse high impedance glow. Full breakdown, characterized by the collapse of the impedance and a rapid increase of 3-4 orders of magnitude in current, is observed to follow the formation of localized radial current channels linking the filament to the electrodes. Breakdown occurs a few hundred ns to a few  $\mu$ s after the arrival of the laser pulse, depending on the laser pulse energy and voltage applied. After breakdown, the increased discharge heating causes the rate of expansion of these arcs and the filament-initiated discharge channel itself to rapidly increase.

The breakdown voltages for discharges initiated by laser filaments generated at 100 Hz and 1 kHz was measured to be practically the same. This is consistent with interferometry and hydrodynamic modeling results which show that the density depression that develops after the arrival of a single laser pulse can reach >75 %, which overwhelms the cumulative density depression measured in a sustained 1 kHz sequence, causing the large measured reduction in the breakdown voltage. The measured magnitude of the density depression caused by a single laser pulse is consistent with that required to observe a > 4 X reduction in breakdown voltage in these dc-biased discharges. However, the effect of the cumulative depression in facilitating breakdown cannot be neglected, as if voltage were to be suddenly applied at any time during a laser pulse train except for the time soon after a laser pulse where the single pulse effect dominates, the cumulative air depression present at high repetition rates (eg. 1 kHz) would lower the breakdown voltage, as reported in the literature [32].

From the point of view of applications, the results obtained demonstrate the stable repetitive generation of discharge channels in the atmosphere at 1 kHz repetition rate, with a record reduction in discharge voltage. The increased understanding of the physics of the formation of laser filament-guided discharges in air at such high repetition rates can be expected to contribute to their use in applications.

**Acknowledgements:** We thank Pierre Gaudin from the University of Rochester for providing the fast-framing camera that was used as part of the diagnostics.

**Funding.** This work was supported by the DOD Office of Naval Research grant N00014-19-1-2254 and by a Vannevar Bush Faculty Fellowship, ONR award N000142012842

## References

1. J. R. Vaill, D. A. Tidman, T. D. Wilkerson, and D. W. Koopman, "Propagation of high-voltage streamers along laser-induced ionization trails," *Appl. Phys. Lett.* **17**, 20–22 (1970).
2. K. A. Saum and D. W. Koopman, "Discharges Guided by Laser-Induced Rarefaction Channels," *Phys. Fluids* **15**, 2077–2079 (1972).
3. J. R. Greig, D. W. Koopman, R. F. Fernsler, R. E. Pechacek, I. M. Vitkovitsky, and A. W. Ali, "Electrical Discharges Guided by Pulsed Co<sub>2</sub> -Laser Radiation," *Phys. Rev. Lett.* **41**, 174–177 (1978).

4. M. Miki, Y. Aihara, and T. Shindo, "Development of long gap discharges guided by a pulsed CO<sub>2</sub> laser," *J. Phys. Appl. Phys.* **26**, 1244–1252 (1993).
5. M. Miki, T. Shindo, and Y. Aihara, "Mechanisms of guiding ability of laser-produced plasmas on pulsed discharges," *J. Phys. Appl. Phys.* **29**, 1984–1996 (1996).
6. T. Shindo, M. Miki, Y. Aihara, and A. Wada, "Laser-guided discharges in long gaps," *IEEE Trans. Power Deliv.* **8**, 2016–2022 (1993).
7. J. P. Wolf, "Short-pulse lasers for weather control," *Rep. Prog. Phys.* **81**, 026001 (2018).
8. D. Strickland and G. Mourou, "Compression of amplified chirped optical pulses," *Opt. Commun.* **56**, 219–221 (1985).
9. A. Braun, G. Korn, X. Liu, D. Du, J. Squier, and G. Mourou, "Self-channeling of high-peak-power femtosecond laser pulses in air," *Opt. Lett.* **20**, 73–75 (1995).
10. B. La Fontaine, F. Vidal, Z. Jiang, C. Y. Chien, D. Comtois, A. Desparois, T. W. Johnston, J.-C. Kieffer, H. Pépin, and H. P. Mercure, "Filamentation of ultrashort pulse laser beams resulting from their propagation over long distances in air," *Phys. Plasmas* **6**, 1615–1621 (1999).
11. A. Couairon and A. Mysyrowicz, "Femtosecond filamentation in transparent media," *Phys. Rep.* **441**, 47–189 (2007).
12. L. Bergé, S. Skupin, R. Nuter, J. Kasparian, and J.-P. Wolf, "Ultrashort filaments of light in weakly ionized, optically transparent media," *Rep. Prog. Phys.* **70**, 1633–1713 (2007).
13. D. Comtois, C. Y. Chien, A. Desparois, F. Génin, G. Jarry, T. W. Johnston, J.-C. Kieffer, B. La Fontaine, F. Martin, R. Mawassi, H. Pépin, F. A. M. Rizk, F. Vidal, P. Couture, H. P. Mercure, C. Potvin, A. Bondiou-Clergerie, and I. Gallimberti, "Triggering and guiding leader discharges using a plasma channel created by an ultrashort laser pulse," *Appl. Phys. Lett.* **76**, 819–821 (2000).
14. H. Pépin, D. Comtois, F. Vidal, C. Y. Chien, A. Desparois, T. W. Johnston, J. C. Kieffer, B. La Fontaine, F. Martin, F. A. M. Rizk, C. Potvin, P. Couture, H. P. Mercure, A. Bondiou-Clergerie, P. Lalande, and I. Gallimberti, "Triggering and guiding high-voltage large-scale leader discharges with sub-joule ultrashort laser pulses," *Phys. Plasmas* **8**, 2532–2539 (2001).
15. D. F. Gordon, A. Ting, R. F. Hubbard, E. Briscoe, C. Manka, S. P. Slinker, A. P. Baronavski, H. D. Ladouceur, P. W. Grounds, and P. G. Girardi, "Streamerless guided electric discharges triggered by femtosecond laser filaments," *Phys. Plasmas* **10**, 4530–4538 (2003).
16. A. Schmitt-Sody, J. Elle, A. Lucero, M. Domonkos, A. Ting, and V. Hasson, "Dependence of single-shot pulse durations on near-infrared filamentation-guided breakdown in air," *AIP Adv.* **7**, 035018 (2017).
17. Y.-H. Chen, S. Varma, T. M. Antonsen, and H. M. Milchberg, "Direct Measurement of the Electron Density of Extended Femtosecond Laser Pulse-Induced Filaments," *Phys. Rev. Lett.* **105**, 215005 (2010).
18. R. P. Fischer, A. C. Ting, D. F. Gordon, R. F. Fernsler, G. P. DiComo, and P. Sprangle, "Conductivity Measurements of Femtosecond Laser-Plasma Filaments," *IEEE Trans. Plasma Sci.* **35**, 1430–1436 (2007).
19. S. Tzortzakis, B. Prade, M. Franco, A. Mysyrowicz, S. Hüller, and P. Mora, "Femtosecond laser-guided electric discharge in air," *Phys. Rev. E* **64**, 057401 (2001).

20. G. Point, C. Milián, A. Couairon, A. Mysyrowicz, and A. Houard, "Generation of long-lived underdense channels using femtosecond filamentation in air," *J. Phys. B At. Mol. Opt. Phys.* **48**, 094009 (2015).
21. E. W. Rosenthal, I. Larkin, A. Goffin, T. Produit, M. C. Schroeder, J.-P. Wolf, and H. M. Milchberg, "Dynamics of the femtosecond laser-triggered spark gap," *Opt. Express* **28**, 24599 (2020).
22. S. Tzortzakis, B. Prade, M. Franco, and A. Mysyrowicz, "Time-evolution of the plasma channel at the trail of a self-guided IR femtosecond laser pulse in air," *Opt. Commun.* **181**, 123–127 (2000).
23. N. Jhajj, E. W. Rosenthal, R. Birnbaum, J. K. Wahlstrand, and H. M. Milchberg, "Demonstration of Long-Lived High-Power Optical Waveguides in Air," *Phys. Rev. X* **4**, 011027 (2014).
24. F. Paschen, "On the potential difference required for spark transfer in air, hydrogen and carbonic acid at different pressures," *Ann Phys* **273**, 69–96 (1889).
25. P. Rambo, J. Schwarz, and J.-C. Diels, "High-voltage electrical discharges induced by an ultrashort-pulse UV laser system," *J. Opt. Pure Appl. Opt.* **3**, 146–158 (2001).
26. M. Rodriguez, R. Sauerbrey, H. Wille, L. Wöste, T. Fujii, Y.-B. André, A. Mysyrowicz, L. Klingbeil, K. Rethmeier, W. Kalkner, J. Kasparian, E. Salmon, J. Yu, and J.-P. Wolf, "Triggering and guiding megavolt discharges by use of laser-induced ionized filaments," *Opt. Lett.* **27**, 772–774 (2002).
27. A. Houard, C. D'Amico, Y. Liu, Y. B. Andre, M. Franco, B. Prade, A. Mysyrowicz, E. Salmon, P. Pierlot, and L.-M. Cleon, "High current permanent discharges in air induced by femtosecond laser filamentation," *Appl. Phys. Lett.* **90**, 171501 (2007).
28. K. Sugiyama, T. Fujii, M. Miki, M. Yamaguchi, A. Zhidkov, E. Hotta, and K. Nemoto, "Laser-filament-induced corona discharges and remote measurements of electric fields," *Opt. Lett.* **34**, 2964–2966 (2009).
29. B. Forestier, A. Houard, I. Revel, M. Durand, Y. B. André, B. Prade, A. Jarnac, J. Carbonnel, M. Le Nevé, J. C. De Miscault, B. Esmler, D. Chapuis, and A. Mysyrowicz, "Triggering, guiding and deviation of long air spark discharges with femtosecond laser filament," *AIP Adv.* **2**, 012151 (2012).
30. K. Guo, J. Lin, Z. Hao, X. Gao, Z. Zhao, C. Sun, and B. Li, "Triggering and guiding high-voltage discharge in air by single and multiple femtosecond filaments," *Opt. Lett.* **37**, 259 (2012).
31. Y.-H. Cheng, J. K. Wahlstrand, N. Jhajj, and H. M. Milchberg, "The effect of long timescale gas dynamics on femtosecond filamentation," *Opt. Express* **21**, 4740–4751 (2013).
32. P. Walch, B. Mahieu, L. Arantchouk, Y.-B. André, A. Mysyrowicz, and A. Houard, "Cumulative air density depletion during high repetition rate filamentation of femtosecond laser pulses: Application to electric discharge triggering," *Appl. Phys. Lett.* **119**, 264101 (2021).
33. J. K. Wahlstrand, N. Jhajj, E. W. Rosenthal, S. Zahedpour, and H. M. Milchberg, "Direct imaging of the acoustic waves generated by femtosecond filaments in air," *Opt. Lett.* **39**, 1290–1293 (2014).
34. Y. Wang, H. Chi, C. Baumgarten, K. Dehne, A. R. Meadows, A. Davenport, G. Murray, B. A. Reagan, C. S. Menoni, and J. J. Rocca, "1.1 J Yb:YAG picosecond laser at 1 kHz repetition rate," *Opt. Lett.* **45**, 6615–6618 (2020).



35. B. A. Reagan, A. H. Curtis, K. A. Wernsing, F. J. Furch, B. M. Luther, and J. J. Rocca, "Development of High Energy Diode-Pumped Thick-Disk Yb:YAG Chirped-Pulse-Amplification Lasers," *IEEE J. Quantum Electron.* **48**, 827–835 (2012).
36. T. Metzger, A. Schwarz, C. Y. Teisset, D. Sutter, A. Killi, R. Kienberger, and F. Krausz, "High-repetition-rate picosecond pump laser based on a Yb:YAG disk amplifier for optical parametric amplification," *Opt. Lett.* **34**, 2123–2125 (2009).
37. T. Produit, P. Walch, G. Schimmel, B. Mahieu, C. Herkommer, R. Jung, T. Metzger, K. Michel, Y.-B. André, A. Mysyrowicz, A. Houard, J. Kasparian, and J.-P. Wolf, "HV discharges triggered by dual- and triple-frequency laser filaments," *Opt. Express* **27**, 11339–11347 (2019).
38. A. Houard, V. Jukna, G. Point, Y.-B. André, S. Klingebiel, M. Schultze, K. Michel, T. Metzger, and A. Mysyrowicz, "Study of filamentation with a high power high repetition rate ps laser at 103  $\mu\text{m}$ ," *Opt. Express* **24**, 7437–7448 (2016).
39. A. Higginson, Y. Wang, H. Chi, A. Goffin, I. Larkin, H. M. Milchberg, and J. J. Rocca, "Wake dynamics of air filaments generated by high-energy picosecond laser pulses at 1 kHz repetition rate," *Opt. Lett.* **46**, 5449–5452 (2021).
40. C. Herkommer, P. Krötz, R. Jung, S. Klingebiel, C. Wandt, R. Bessing, P. Walch, T. Produit, K. Michel, D. Bauer, R. Kienberger, and T. Metzger, "Ultrafast thin-disk multipass amplifier with 720 mJ operating at kilohertz repetition rate for applications in atmospheric research," *Opt. Express* **28**, 30164 (2020).
41. A. Houard, P. Walch, T. Produit, V. Moreno, B. Mahieu, A. Sunjerga, C. Herkommer, A. Mostajabi, U. Andral, Y.-B. André, M. Lozano, L. Bizet, M. C. Schroeder, G. Schimmel, M. Moret, M. Stanley, W. A. Rison, O. Maurice, B. Esmiller, K. Michel, W. Haas, T. Metzger, M. Rubinstein, F. Rachidi, V. Cooray, A. Mysyrowicz, J. Kasparian, and J.-P. Wolf, "Laser-guided lightning," *Nat. Photonics* **17**, 231–235 (2023).
42. H. Raether, *Electron Avalanches and Breakdown in Gases* (Butterworths, 1964).
43. J. M. Meek and J. D. Craggs, eds., *Electrical Breakdown of Gases*, Wiley Series in Plasma Physics (Wiley, 1978).
44. J. A. Rees, *Electrical Breakdown in Gases* (Wiley, 1973).
45. G. Schaefer, ed., *Gas Discharge Closing Switches* (Plenum Press, 1990).
46. Ref[43], Pages 539-545 (n.d.).
47. E. Marode, "The mechanism of spark breakdown in air at atmospheric pressure between a positive point and plane. II. Theoretical: Computer simulation of the streamer track," *J. Appl. Phys.* **46**, 2016–2020 (1975).
48. Yu. V. Afanas'ev, V. P. Avtonomov, N. G. Basov, G. Korn, G. V. Sklizkov, and V. N. Shlyaptsev, "Radiative transport in a laser plasma," *J. Sov. Laser Res.* **10**, 1–13 (1989).
49. E. Marode, F. Bastien, and M. Bakker, "A model of the streamer-induced spark formation based on neutral dynamics," *J. Appl. Phys.* **50**, 140–146 (1979).
50. W. A. Gambling and H. Edels, "The high-pressure glow discharge in air," *Br. J. Appl. Phys.* **5**, 36–39 (1954).
51. R. H. Stark and K. H. Schoenbach, "Direct current high-pressure glow discharges," *J. Appl. Phys.* **85**, 2075–2080 (1999).